Viatcheslav S. LOVEIKIN [1], Yuriy O. ROMASEVYCH [1],
Andriy V. LOVEIKIN [2], Mykola M. KOROBKO [1],
Anastasia P. LIASHKO [1]

Minimization of oscillations of the tower crane slewing mechanism in the steady-state mode of trolley movement

In the present study, the problem of optimization of the motion mode of the tower crane's slewing mechanism in the steady-state mode of trolley movement is stated and solved. An optimization criterion, which includes the RMS values of the drive torque and the rate of its change over time, is minimized. The optimization is carried out taking into account the drive torque constraints, and under the specified boundary conditions of motion. Three optimization problems at different values of the weight coefficients are solved. In the first problem, priority is given to the drive torque, in the third – to the rate of the drive torque change, and in the second problem, the significance of both components is assumed equal.

The optimization problems are nonlinear, thus a VCT-PSO method is applied to solve them. The obtained optimal start-up modes of the crane slewing mechanism eliminate pendulum load oscillations and high-frequency elastic oscillations of the tower.

Most of the kinematic, dynamical, and power parameters at different values of the weight coefficients are quite close to each other. It indicates that the optimal modes of motion are significantly influenced by the boundary conditions, optimization parameters, and constraints.

✉ Yuriy ROMASEVYCH, e-mail: romasevichyuriy@ukr.net

[1]National University of Life and Environmental Sciences of Ukraine, Kyiv, Ukraine. ORCIDs: V.S.L. 0000-0003-4259-3900; Y.O.R. 0000-0001-5069-5929; M.M.K. 0000-0002-2602-4225; A.P.L. 0000-0002-3774-3348

[2]Taras Shevchenko National University of Kyiv, Kyiv, Ukraine. ORCID: 0000-0002-7988-8350

1. Introduction

When using tower cranes, in order to increase the capacity of loading and unloading operations, one must amend the mechanisms for trolley movement and slewing. However, in this case, dynamical loads increase in the structural elements of the crane and drive mechanisms, which leads to a decrease in the accuracy of load handling operations and crane reliability, as well as increased energy losses. Particularly dangerous are the loads caused by low-frequency oscillations of the load on the flexible suspension and high-frequency oscillations of the crane structure and drive mechanisms. One of the modes of joint operation of the mechanisms is the mode when the trolley moves in a steady-state mode, and the slewing mechanism operates in a transient process (start, braking, change of motion speed). In this mode of joint motion of the mechanisms, there is a need to minimize oscillations in the elements of the crane structure and the load. The oscillations of structural elements and load are significantly affected by the magnitude and the change in the drive torque of the slewing mechanism during transient processes. In particular, the rate of change of the drive torque is important in this case. Therefore, the problem is to choose a favorable mode of change of the drive torque of the slewing mechanism during startup or braking, which would minimize oscillations in the crane structure elements.

When using hoisting cranes, in order to increase the capacity of transport and technological operations, the operation of several mechanisms is involved [1–6]. For example, during the operation of tower cranes, the load performs a complex motion in which several mechanisms function simultaneously. The operation of these mechanisms has both a mutual and a general effect on the crane structure [1]. This requires the operator to be precise in choosing the operating modes of crane mechanisms. Therefore, there is a need to improve the mechanisms operating control efficiency. This increases the dynamical loads in the elements of drive mechanisms and crane structures, as well as the oscillations of the load on a flexible suspension [4–7]. Researchers from different countries have paid considerable attention to the study of dynamical processes in the elements of hoisting machines [8–11]. The studies [8, 9] researched the dynamics of trolley movement. In the paper [12], dynamics of hoisting operation of bridge crane was investigated.

The studies [4, 5] consider the joint motion of the mechanisms for trolley movement and slewing of hoisting cranes, in particular tower cranes. In this case, the drive of the mechanism for trolley movement during crane slewing with a suspended load on a flexible suspension is controlled to reduce its oscillations. Studies [6, 7] investigated the dynamics of the joint motion of the mechanisms for trolley movement and slewing of a tower crane, where the impact of each mechanism on the dynamics of the crane's motion as a whole was determined. Based on these studies, the kinematic, power, and energy parameters of the mechanisms are determined. In particular, significant power overloads of the drive mechanisms and spatial oscillations of the load are detected.

In order to reduce the oscillations of the load on a flexible suspension, optimization problems of motion modes during the operation of individual mechanisms are solved in many scientific studies. For instance, in the work [13], the transient process of the startup of the trolley movement mechanism is optimized by controlling the drive torque to minimize dynamical loads. Study [14] presents a solution to the problem of optimizing the mode of motion of the trolley movement mechanism of a tower crane in a steady-state slewing mode.

In the study [15] load oscillations elimination, accurate slew/translation positioning of the trolley and the jib, and duration minimization are the goal to reach. In this paper, a new suboptimal trajectory planning method is proposed for 4-DOF tower crane system, eight constraints are involved in the problem statement as well. The solution of the problem is compared with LQR results and validated through experiments on the lab installation.

Both open-loop [6, 9–11, 13–15] and closed-loop [16–19] controls are involved in the problem of load oscillations elimination.

In the article [16], the joint application of feedback control (active method) and a damper (passive method) on a load cable is considered. Such an approach allowed for combining the positive features of each of the methods. Optimal parameters of the spring-damper system are obtained. The performance of the proposed scheme is illustrated via numerical simulations for various cases of initial angle, initial velocity, drive acceleration, and control gain.

In the work [17], a nonlinear mathematical model of a robotic tower crane is derived. Based on the linearization of the model (at each iteration of the control algorithm around its present operating point), the authors stated and solved the H_∞ control problem. A strong feature of this work consists in the advantages of the linear optimal control (fast and accurate tracking of reference setpoints), the weaknesses – are the quite a big amount of computations that must be performed on each control iteration and the absence of constraints imposed on control and state vector components. In addition, the stability of the control is proven via Lyapunov analysis.

Article [18] proposes an approach to suppressing load oscillations in radial and tangential directions. To reach the goal, one uses a nonlinear model of the tower crane, and four constraints are imposed on the kinematical functions of the system. The authors applied a smooth command input shaper and optimized its parameters with a particle swarm algorithm. Lab experiments supported the theoretical results. However, there is no optimization during the movement, only at the final moment of movement.

Paper [19] presents the ODE-PDE mathematical model of the tower crane, where its rotation and trolley movement are considered. PDE is used to describe the oscillations of the crane jib. The objective function to minimize is a combination of the duration of the controlled process, the kinetic energy of the load, control force, and penalty terms, which are related to the final conditions. Some numerical calculations and their brief analysis are given to support strong theoretical results.

All of these works support the idea that the problem of determination of the transient mode of crane slewing at a steady trolley movement remains important.

Then, the goal of the present study is to minimize oscillations of tower crane structural elements by optimizing the start-up mode of the slewing drive mechanism at a steady-state trolley movement.

2. Optimization Problem Statement

For the purpose of the study, the tower crane boom system during the joint motion of the slewing and trolley movement mechanisms (Fig. 1) is presented as a holonomic mechanical system consisting of absolutely rigid links, except for the crane rotary part 1, which has elastic properties with a stiffness coefficient C and the flexible suspension 2 of the load 3, which deviates from the vertical by an angle υ when the crane is rotated. In the accepted dynamical model of the tower crane boom system, the applied generalized coordinates are the angular coordinates of the slewing mechanism drive α, the crane rotary part with boom φ and the load on the flexible suspension ψ, as well as the linear coordinate of the trolley's center of mass x.
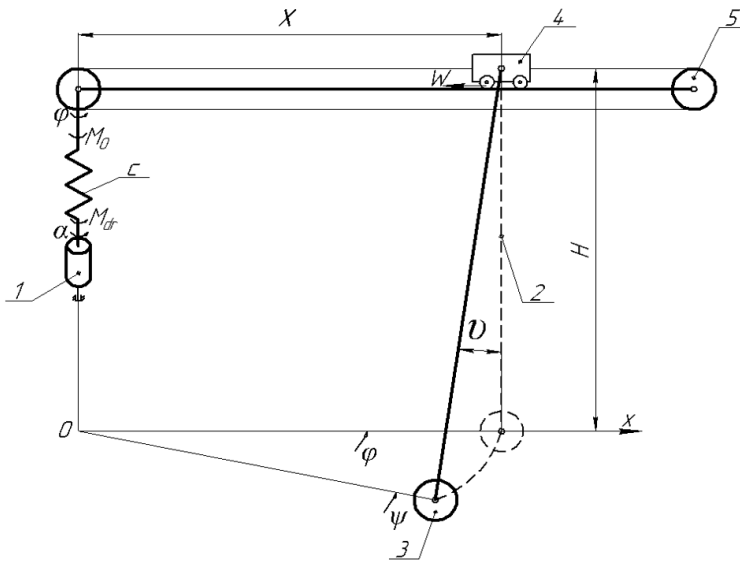
Fig. 1. Dynamical model of the joint motion of crane slewing and trolley movement mechanisms

The trolley 4 with the load 3 moves along the boom 5 with a constant speed V, and the length of the flexible load suspension remains constant and equals H Since the trolley moves at a constant speed, the coordinate x is determined by the following dependence

$$x = x_0 + Vt, \tag{1}$$

where t is time; x_0 is initial trolley position along the boom.

Since the linear coordinate of the trolley x is known, the dynamical model of the boom system has three degrees of freedom. The flexible load suspension deviates from the vertical by an angle

$$\upsilon = \frac{x}{H}(\varphi - \psi). \tag{2}$$

Based on the dynamical model (Fig. 1) Lagrange's second order equations are used to derive differential equations of motion as follows:

$$I_1\ddot{\alpha} = M_{dr} - C(\alpha - \varphi),$$

$$\left(I_0 + m_0(x_0 + Vt)^2\right)\ddot{\varphi} + 2m_0V(x_0 + Vt)^2\dot{\varphi}$$

$$= -M_0 + C(\alpha - \varphi) + \frac{mg}{H}(x_0 + Vt)^2(\varphi - \psi), \tag{3}$$

$$(x_0 + Vt)\ddot{\psi} + 2V\dot{\psi} = \frac{g}{H}(x_0 + Vt)^2(\varphi - \psi),$$

where I_1, I_0 – crane rotary part and slewing mechanism drive moments of inertia, reduced to the crane rotary axis respectively; m_0, m– trolley and load masses respectively; M_{dr}, M_0 – the drive torque of the slewing mechanism and the torque caused by the resistance of the rotary crane part, reduced to the crane rotary axis respectively; g – the acceleration of gravity.

High-frequency oscillations of the slewing mechanism elements and low-frequency oscillations of the flexibly suspended load significantly depend on the drive torque and the rate of its change over time during non-steady motion of the mechanism (acceleration or deceleration). Therefore, let us choose a non-dimensional complex criterion, including RMS of the drive torque and the rate of drive torque change during acceleration, as an optimization criterion which is common for such problems [6]:

$$Cr = Cr_1\delta_1 + Cr_2\delta_2 + Ineq = \delta_1 \frac{\sqrt{\dfrac{1}{t_1}\displaystyle\int_0^{t_1} M_{dr}^2\,\mathrm{d}t}}{\min\left(\sqrt{\dfrac{1}{t_1}\displaystyle\int_0^{t_1} M_{dr}^2\,\mathrm{d}t}\right)}$$

$$+ \delta_2 \frac{\sqrt{\dfrac{1}{t_1}\displaystyle\int_0^{t_1} \dot{M}_{dr}^2\,\mathrm{d}t}}{\min\left(\sqrt{\dfrac{1}{t_1}\displaystyle\int_0^{t_1} \dot{M}_{dr}^2\,\mathrm{d}t}\right)} + Ineq \rightarrow \min; \tag{4}$$

$$\delta_1 + \delta_2 = 1,$$

where δ_1 and δ_2 are weight coefficients that show the importance of minimization of each component of the complex criterion, t_1 – duration of the slewing mechanism startup process; $\dot{M}_{dr} = \mathrm{d}M_{dr}/\mathrm{d}t$ – the rate of the slewing mechanism drive torque change over time; $Ineq$ – penalty component of the criterion that correspond to the drive torque constraints $0 \leqslant M_{dr} \leqslant M_{\max.dr}$ and defined as follows:

$$
Ineq = \begin{cases} 0, & \text{if } M_{\max.dr} \geqslant M_{dr} \geqslant 0; \\[2ex] \dfrac{\max\left(|\min(M_{dr})|,\ \max(M_{dr})\right)}{\min\left(\sqrt{\dfrac{1}{t_1}\displaystyle\int_0^{t_1} M_{dr}^2\,\mathrm{d}t}\right)}\delta_{ineq}, & \text{if } \begin{array}{l} M_{dr} < 0\ \vee \\ M_{dr} > M_{\max.dr} \end{array} \end{cases}, \qquad (5)
$$

where δ_{ineq} is a penalty coefficient that affects the increase of the value of $Ineq$, if the constraints $0 \leqslant M_{dr} \leqslant M_{\max.dr}$ are violated; $M_{\max.dr}$ is a maximum value of the drive torque (in this study, it is set as $M_{\max.dr} = 200$ kNm).

The first term of criterion (4) allows for minimizing the equivalent drive torque, which, in turn, minimizes energy losses in the drive. Minimization of the second term has a positive effect on the smoothness of the crane motion as well as the reducing of the dynamical impacts in the crane metal structure.

3. Optimization Problem Solving

Note that in order to find the denominators of the first and second terms of criterion (4), the following optimization problems must be solved:

$$
\min\left(\sqrt{\frac{1}{t_1}\int_0^{t_1} M_{dr}^2\,\mathrm{d}t}\right) + Ineq \rightarrow \min,
$$

$$
\min\left(\sqrt{\frac{1}{t_1}\int_0^{t_1} \dot{M}_{dr}^2\,\mathrm{d}t}\right) + Ineq \rightarrow \min. \qquad (6)
$$

Thus, criterion (4) specifies the requirements for the fulfillment of constraints $0 \leqslant M_{dr} \leqslant M_{\max.dr}$, minimization of the RMS value of the drive torque and its rate of change over time. The latter two requirements are met on a compromise basis.

The minimization of the complex criterion (4) and the denominators of its terms (6) is carried out when the boundary conditions of the system motion are

satisfied:

$$t = 0: \quad \psi = 0; \quad \dot{\psi} = 0; \quad \varphi = 0; \quad \dot{\varphi} = 0; \quad \alpha = \frac{M_0}{C}; \quad \dot{\alpha} = 0; \quad \ddot{\alpha} = \ddot{\alpha}_0; \quad \dddot{\alpha} = \dddot{\alpha}_0;$$

$$t = t_1: \quad \psi = \frac{\omega t_1}{2}; \quad \dot{\psi} = \omega; \quad \varphi = \frac{\omega t_1}{2}; \quad \dot{\varphi} = \omega; \quad \alpha = \frac{M_0}{C} + \frac{\omega t_1}{2}; \tag{7}$$

$$\dot{\alpha} = \omega; \quad \ddot{\alpha} = \ddot{\alpha}_{t_1}; \quad \dddot{\alpha} = \dddot{\alpha}_{t_1},$$

where ω – crane rotary part steady motion angular velocity; $\ddot{\alpha}_0$, $\ddot{\alpha}_{t_1}$ – angular accelerations of the drive slewing mechanism at the beginning and at the end of the startup process, respectively; $\dddot{\alpha}_0$, $\dddot{\alpha}_{t_1}$ – angular jerks of the drive slewing mechanism at the beginning and at the end of the startup process, respectively. First six final conditions mean elimination of the system oscillations at the end of the acceleration (slewing mechanism drive, crane rotary part with boom and load on the flexible suspension must be at the same position and move at the angular speed ω; the pendulum load oscillations must be eliminated in the plane, which is perpendicular to the boom). Boundary conditions $\ddot{\alpha}_0$, $\ddot{\alpha}_{t_1}$, $\dddot{\alpha}_0$, $\dddot{\alpha}_{t_1}$ are unknown parameters that need to be determined in order to optimize the startup mode of the slewing mechanism.

From the first equation of the system (3), we derive the expression of the drive torque

$$M_{dr} = I_1 \ddot{\alpha} + C(\alpha - \varphi). \tag{8}$$

By taking the time derivative of expression (8), we determine the rate of the drive torque change

$$\dot{M}_{dr} = I_1 \dddot{\alpha} + C(\dot{\alpha} - \dot{\varphi}). \tag{9}$$

Dependencies (8) and (9) include the coordinates of the slewing mechanism drive α and the crane rotary part φ. We express them in terms of the generalized coordinate of the load's rotation ψ and its time derivatives. For this purpose, from the last equation of system (3), we express the generalized coordinate of the crane rotary part

$$\varphi = \psi + \left(\ddot{\psi} + 2V \frac{\dot{\psi}}{x_0 + Vt} \right) \frac{H}{g}. \tag{10}$$

From the second equation of system (3), we find the generalized coordinate of the slewing mechanism drive

$$\alpha = \varphi + \frac{1}{C} \left(\left(I_0 + m_0(x_0 + Vt)^2 \right) \ddot{\varphi} + 2m_0(x_0 + Vt)V\dot{\varphi} \right.$$
$$\left. + m(x_0 + Vt)^2 \ddot{\psi} + 2m(x_0 + Vt)V\dot{\psi} + M_0 \right). \tag{11}$$

The dependence of the drive torque (8) and the rate of its change over time (9) includes time derivatives of the generalized coordinate of the drive mechanism,

thus we should define them:

$$
\dot{\alpha} = \dot{\varphi} + \frac{1}{C}\left(\left(I_0 + m_0(x_0 + Vt)^2\right)\ddot{\varphi} + 4m_0(x_0 + Vt)V\ddot{\varphi} + 2m_0V^2\dot{\varphi}\right.
$$
$$
\left. + m(x_0 + Vt)^2\ddot{\psi} + 4m(x_0 + Vt)V\ddot{\psi} + 2mV^2\dot{\psi}\right), \tag{12}
$$

$$
\ddot{\alpha} = \ddot{\varphi} + \frac{1}{C}\left(\left(I_0 + m_0(x_0 + Vt)^2\right)\overset{\text{IV}}{\varphi} + 6m_0(x_0 + Vt)V\dddot{\varphi} + 6m_0V^2\ddot{\varphi}\right.
$$
$$
\left. + m(x_0 + Vt)^2\overset{\text{IV}}{\psi} + 6m(x_0 + Vt)V\dddot{\psi} + 6mV^2\ddot{\psi}\right), \tag{13}
$$

$$
\dddot{\alpha} = \dddot{\varphi} + \frac{1}{C}\left(\left(I_0 + m_0(x_0 + Vt)^2\right)\overset{\text{V}}{\varphi} + 8m_0(x_0 + Vt)V\overset{\text{IV}}{\varphi} + 12m_0V^2\dddot{\varphi}\right.
$$
$$
\left. + m(x_0 + Vt)^2\overset{\text{V}}{\psi} + 8m(x_0 + Vt)V\overset{\text{IV}}{\psi} + 12mV^2\dddot{\psi}\right). \tag{14}
$$

Dependencies (9)–(14) include time derivatives of the function $\varphi(t)$ up to the fifth order, so we determine them by using expression (10):

$$
\dot{\varphi} = \dot{\psi} + \frac{H}{g}\left(\dddot{\psi} + 2V\frac{\ddot{\psi}(x_0 + Vt) - V\dot{\psi}}{(x_0 + Vt)^2}\right), \tag{15}
$$

$$
\ddot{\varphi} = \ddot{\psi} + \frac{H}{g}\left(\overset{\text{IV}}{\psi} + 2V\frac{\dddot{\psi}(x_0 + Vt)^2 - 2V(x_0 + Vt)\ddot{\psi} + 2V^2\dot{\psi}}{(x_0 + Vt)^3}\right), \tag{16}
$$

$$
\dddot{\varphi} = \dddot{\psi} + \frac{H}{g}\left(\overset{\text{V}}{\psi} + \frac{2V}{(x_0 + Vt)^4}\left(\overset{\text{IV}}{\psi}(x_0 + Vt)^3 - 3V(x_0 + Vt)^2\dddot{\psi}\right.\right.
$$
$$
\left.\left. + 6V^2(x_0 + Vt)^2\ddot{\psi} - 6V^3\dot{\psi}\right)\right), \tag{17}
$$

$$
\overset{\text{IV}}{\varphi} = \overset{\text{IV}}{\psi} + \frac{H}{g}\left(\overset{\text{VI}}{\psi} + \frac{2V}{(x_0 + Vt)^5}\left(\overset{\text{V}}{\psi}(x_0 + Vt)^4 - 4V(x_0 + Vt)^3\overset{\text{IV}}{\psi}\right.\right.
$$
$$
\left.\left. + 12V^2(x_0 + Vt)^2\dddot{\psi} - 24V^2(x_0 + Vt)\ddot{\psi} + 24V^4\dot{\psi}\right)\right), \tag{18}
$$

$$
\overset{\text{V}}{\varphi} = \overset{\text{V}}{\psi} + \frac{H}{g}\left(\overset{\text{VII}}{\psi} + \frac{2V}{(x_0 + Vt)^6}\left(\overset{\text{VI}}{\psi}(x_0 + Vt)^5 - 5V(x_0 + Vt)^4\overset{\text{V}}{\psi}\right.\right.
$$
$$
\left.\left. + 20V^2(x_0 + Vt)^3\overset{\text{IV}}{\psi} - 60V^3(x_0 + Vt)\dddot{\psi} + 120V^4(x_0 + Vt)\ddot{\psi}\,120V^5\dot{\psi}\right)\right). \tag{19}
$$

In this optimization problem, we express the boundary conditions (7) in terms of the generalized angular coordinate of the load rotation and its time derivatives.

First, let's consider the initial startup time ($t = 0$). From the initial conditions (6), we find that $\psi(0) = 0$ and $\dot{\psi}(0) = 0$. Taking into account that $\varphi(0) = 0$, $\dot{\varphi}(0) = 0$ and considering dependencies (10) and (15), we find that $\ddot{\psi}(0) = 0$, $\dddot{\psi}(0) = 0$. Also, from the initial startup conditions, we have $\alpha = \dfrac{M_0}{C}$, $\dot{\alpha} = 0$. Thus, we find from dependence (11) that $\ddot{\varphi}(0) = 0$. Then, from dependence (16) we have

that $\overset{\text{IV}}{\psi}(0) = 0$. From the boundary condition $\dot{\alpha}(0) = 0$, using the dependence (13), we determine that $\dddot{\varphi}(0) = 0$. From this condition, by expression (17), we derive that

$$\overset{\text{V}}{\psi}(0) = 0.$$

From the boundary condition $\ddot{\alpha}(0) = \ddot{\alpha}_0$ using dependence (13), we determine that

$$\overset{\text{IV}}{\varphi}(0) = \frac{C\ddot{\alpha}_0}{I_0 + m_0 x_0^2} \, . \tag{20}$$

From the obtained condition (20), using expression (18), we find that the sixth time derivative of the angular coordinate of the load's rotation is determined by the following dependence

$$\overset{\text{VI}}{\psi}(0) = \frac{g}{H} \frac{C\ddot{\alpha}_0}{I_0 + m_0 x_0^2} \, . \tag{21}$$

From the boundary condition $\dddot{\alpha}(0) = \dddot{\alpha}_0$, using dependence (14), we have

$$\overset{\text{V}}{\varphi}(0) = \frac{C\ddot{\alpha}_0}{I_0 + m_0 x_0^2} \left(\dddot{\alpha}_0 - \frac{8 m_0 x_0 V}{I_0 + m_0 x_0^2} \ddot{\alpha}_0 \right) . \tag{22}$$

From condition (22), using expression (19), we find the seventh time derivative of the angular coordinate of the load slewing at the moment of time when

$$\overset{\text{VII}}{\psi}(0) = \frac{g}{H} \frac{C\ddot{\alpha}_0}{I_0 + m_0 x_0^2} \left(\dddot{\alpha}_0 - \left(\frac{8 m_0 x_0 V}{I_0 + m_0 x_0^2} + \frac{2V}{x_0} \right) \ddot{\alpha}_0 \right) . \tag{23}$$

Let's consider the final moment of time, when $t = t_1$. From the startup boundary conditions (7) we have $\psi(t_1) = \frac{\omega t_1}{2}$ and $\dot{\psi}(t_1) = \omega$. Also, from the startup boundary conditions, it is known that $\varphi(t_1) = \frac{\omega t_1}{2}$ and $\dot{\varphi}(t_1) = \omega$. Then, from expressions (10) and (12), we determine:

$$\dddot{\psi}(t_1) = -\frac{2V\omega}{x_0 + Vt_1} \, , \qquad \ddddot{\psi}(t_1) = 6 \frac{V^2 \omega}{(x_0 + Vt_1)^2} \, . \tag{24}$$

Taking into account the condition at the end of the startup, when the drive coordinate is $\alpha(t_1) = \frac{M_0}{C} + \frac{\omega t_1}{2}$, from dependence (9), we determine the expression of the second time derivative of the angular coordinate of the crane rotary part at the end of the startup

$$\ddot{\varphi}(t_1) = -\frac{2 m_0 (x_0 + Vt_1) V\omega}{I_0 + m_0 (x_0 + Vt_1)^2} \, . \tag{25}$$

Now, using expression (21) from dependence (14), we find the fourth time derivative of the angular coordinate of the load at $t = t_1$

$$\overset{IV}{\psi}(t_1) = \frac{2gV\omega}{H(x_0 + Vt_1)}\left(1 - \frac{m_0}{m_0 + \dfrac{I_0}{(x_0 + Vt_1)^2}}\right) - \frac{24V^3\omega}{(x_0 + Vt_1)^3}. \tag{26}$$

Taking into account the condition of $\dot{\alpha}(t_1) = \omega$, from dependence (10) we derive the expression of the third time derivative of the angular coordinate of the crane rotary part at the end of the startup

$$\dddot{\varphi}(t_1) = \frac{2m_0V^2\omega}{I_0 + m_0(x_0 + Vt_1)^2}\left(\frac{4m_0(x_0 + Vt_1)^2}{I_0 + m_0(x_0 + Vt_1)^2} - 1\right). \tag{27}$$

From the obtained condition (27), using expression (17), we determine the fifth time derivative of the angular coordinate of the load rotation

$$\begin{aligned}
\overset{v}{\psi}(t_1) &= \frac{2gV^2\omega}{H} \cdot \frac{m_0}{I_0 + m_0(x_0 + Vt_1)^2}\left(1 + \frac{4m_0(x_0 + Vt_1)^2}{I_0 + m_0(x_0 + Vt_1)^2}\right) \\
&+ \frac{10V^2\omega}{(x_0 + Vt_1)^2}\left(\frac{12V^2}{(x_0 + Vt_1)^2} - \frac{g}{H}\right).
\end{aligned} \tag{28}$$

From the boundary condition $\ddot{\alpha}(t_1) = \ddot{\alpha}_{t_1}$, using dependence (13), we determine that

$$\begin{aligned}
\overset{IV}{\varphi}(t_1) &= \frac{1}{I_0 + m_0(x_0 + Vt_1)^2}\left(C\ddot{\alpha}_{t_1} - m(x_0 + Vt_1)^2\overset{IV}{\psi}(t_1)\right. \\
&- 6V(x_0 + Vt_1)\left(m\dddot{\psi}(t_1) + m_0\dddot{\varphi}(t_1)\right) - 6mV^2\ddot{\psi}(t_1) \\
&- \left.\left(6m_0V^2 + C\right)\ddot{\varphi}(t_1)\right).
\end{aligned} \tag{29}$$

From the obtained condition (29), using expression (18), we find that the sixth time derivative of the angular coordinate of the load's rotation is determined by the following dependence

$$\begin{aligned}
\overset{VI}{\psi}(t_1) &= \left(\overset{IV}{\varphi}(t_1) - \overset{IV}{\psi}(t_1)\right)\frac{g}{H} - \frac{V}{(x_0 + Vt_1)^5}\left((x_0 + Vt_1)^4\overset{v}{\psi}(t_1)\right. \\
&- 4V(x_0 + Vt_1)^3\overset{IV}{\psi}(t_1) + 12V^2\left((x_0 + Vt_1)^2\dddot{\psi}(t_1)\right. \\
&- \left.\left.2V(x_0 + Vt_1)\ddot{\psi}(t_1) + 2V^2\omega\right)\right).
\end{aligned} \tag{30}$$

From the boundary condition $\ddot{\alpha}(t_1) = \ddot{\alpha}_{t_1}$, using dependence (15), we have

$$
\overset{IV}{\varphi}(t_1) = \frac{1}{I_0 + m_0(x_0 + Vt_1)^2} \left(C\ddot{\alpha}_{t_1} - m(x_0 + Vt_1)^2 \overset{V}{\psi}(t_1) \right.
$$
$$
- 8V(x_0 + Vt_1) \left(m \overset{IV}{\psi}(t_1) + m_0 \overset{IV}{\varphi}(t_1) \right)
$$
$$
\left. - \left(12m_0V^2 + C \right) \overset{...}{\varphi}(t_1) - 12mV^2\overset{...}{\psi}(t_1) \right). \tag{31}
$$

From condition (31), using expression (19), we find the seventh time derivative of the angular coordinate of the load slewing at the final moment of time ($t = t_1$):

$$
\overset{VII}{\psi}(t_1) = \left(\overset{V}{\varphi}(t_1) - \overset{V}{\psi}(t_1) \right) \frac{g}{H} - \frac{2V}{(x_0 + Vt_1)^6} \left((x_0 + Vt_1)^5 \overset{VI}{\psi}(t_1) \right.
$$
$$
- 5V(x_0 + Vt_1)^4 \overset{V}{\psi}(t_1) + 20V^2(x_0 + Vt_1)^3 \overset{IV}{\psi}(t_1)
$$
$$
\left. - 60V^3(x_0 + Vt_1)^2 \overset{...}{\psi}(t_1) - 120V^4(x_0 + Vt_1)\ddot{\psi}(t_1) - 120V^5\omega \right). \tag{32}
$$

Thus, taking into account expressions (5)–(32), the minimization of the criterion (4) is carried out when the following boundary conditions for the load rotation are satisfied:

$$
\begin{aligned}
t = 0: \quad & \psi = 0, \ \dot{\psi} = 0, \ \ddot{\psi} = 0, \ \overset{...}{\psi} = 0, \ \overset{IV}{\psi} = 0, \ \overset{V}{\psi} = 0, \\
& \overset{VI}{\psi} = \overset{VI}{\psi}(0), \ \overset{VII}{\psi} = \overset{VII}{\psi}(0), \\
t = t_1: \quad & \psi = \frac{\omega t_1}{2}, \ \dot{\psi} = \omega, \ \ddot{\psi} = \ddot{\psi}(t_1), \ \overset{...}{\psi} = \overset{...}{\psi}(t_1), \\
& \overset{IV}{\psi} = \overset{IV}{\psi}(t_1), \ \overset{V}{\psi} = \overset{V}{\psi}(t_1), \ \overset{VI}{\psi} = \overset{VI}{\psi}(t_1), \ \overset{VII}{\psi} = \overset{VII}{\psi}(t_1).
\end{aligned} \tag{33}
$$

The last two boundary conditions at $t = 0$ are determined by dependencies (21) and (23), and the last six conditions at $t = t_1$ are determined by formulas (24), (26), (28), (30) and (32).

The purpose of such a detailed explanation of calculations (8)–(32) is to allow understanding the way of reducing the initial boundary conditions (7) to those expressed by (33) – suitable for only $\psi(t)$ function operation.

One cannot expect that the optimization problem (4), (33), taking into account expressions (5)–(32), can be solved analytically, due to its nonlinearity, which is caused by the component (5). Therefore, we should solve it approximately. For this purpose, we define a base function that includes free parameters. It is obtained as

a solution to the following three-point boundary problem:

$$L(\psi) = 0;$$

$$t = 0: \quad \psi = 0, \quad \dot{\psi} = 0, \quad \ddot{\psi} = 0, \quad \dddot{\psi} = 0, \quad \overset{IV}{\psi} = 0, \quad \overset{V}{\psi} = 0,$$

$$\overset{VI}{\psi} = \overset{VI}{\psi}(0), \quad \overset{VII}{\psi} = \overset{VII}{\psi}(0);$$

$$\psi\left(\frac{t_1}{2}\right) = \psi_{\frac{t_1}{2}}, \quad \dot{\psi}\left(\frac{t_1}{2}\right) = \dot{\psi}_{\frac{t_1}{2}};$$

$$t = t_1: \quad \psi = \frac{\omega t_1}{2}, \quad \dot{\psi} = \omega, \quad \ddot{\psi} = \ddot{\psi}(t_1), \quad \dddot{\psi} = \dddot{\psi}(t_1), \quad \overset{IV}{\psi} = \overset{IV}{\psi}(t_1),$$

$$\overset{V}{\psi} = \overset{V}{\psi}(t_1), \quad \overset{VI}{\psi} = \overset{VI}{\psi}(t_1), \quad \overset{VII}{\psi} = \overset{VII}{\psi}(t_1).$$

(34)

where $L(\psi)$ is the operator that acts on the function $\psi(t)$ (within this study $L(\psi(t)) = \overset{XVI}{\psi}(t)$); $\ddot{\alpha}_0$, $\dddot{\alpha}_0$, $\psi_{\frac{t_1}{2}}$, $\dot{\psi}_{\frac{t_1}{2}}$, $\ddot{\alpha}_{t_1}$, $\dddot{\alpha}_{t_1}$ – are unknown free parameters of the solution of the boundary problem (34), by which an approximate solution to the original problem (4), (33) is sought.

As a result, the original problem (4), (33) is reduced to the following unconstrained optimization problem:

$$C_r = C_r \left(\ddot{\alpha}_0, \dddot{\alpha}_0, \psi_{\frac{t_1}{2}}, \dot{\psi}_{\frac{t_1}{2}}, \ddot{\alpha}_{t_1}, \dddot{\alpha}_{t_1} \right) \tag{35}$$

Since the problem of optimization of the modes of joint motion of the crane slewing and trolley movement mechanisms is quite complicated and nonlinear, a metaheuristic optimization method VCT-PSO [20] is applied to solve it.

The method VCT-PSO is one of the simple PSO modification. In order to improve canonical PSO method performance it is proposed in the work [20] to change cognitive term in the expression of particles update velocity:

$$v' = wv + c_1 r_1 (\tilde{p} - x) + c_2 r_2 (g - x), \tag{36}$$

where x and v – are position and velocity vectors of a particle ($x \in [x_1, x_2, \ldots, x_i, \ldots, x_D]$; $v \in [v_1, v_2, \ldots, v_i, \ldots, v_D]$); D – is a number of unknown arguments to find ($D = 6$ for considered case); $\tilde{p}$ is the so-called personal best – the best solution, that a particle has found for some number of iterations or the personal best of another (randomly chosen) particle for the rest of iterations; g is the so-called global best – the best solution that a swarm has found; w, c_1 and c_2 are inertial, cognitive and social coefficients, respectively; r_1, r_2 are random numbers that are generated on the interval [0, 1]. The stroke in the superscript means a new position and velocity of a particle. After application of formulas (36), $\tilde{p}$ and g must be updated:

$$\begin{cases} \tilde{p}' = x', & \text{if } f(x') < f(\tilde{p}'); \\ g' = \tilde{p}', & \text{if } f(\tilde{p}') < f(g'), \end{cases} \tag{37}$$

where f is an objective function (in the considered case (35)) to minimize.

All the calculations are performed in the Wolfram Mathematica software.

The quest for solution of the optimization problem of the transient process of the slewing mechanism motion at the steady mode of the trolley movement is performed with the following parameters of the tower crane QTZ-80 system: $m = 5000$ kg, $m_0 = 300$ kg, $I_0 = 4.92 \cdot 10^6$ kg m^2, $I_1 = 5.51 \cdot 10^5$ kg m^2, $V = 0.85$ m/s, $\omega = 0.075$ rad/s, $M_0 = 39890$ Nm, $H = 10$ m, $g = 9.81$ m/s^2, $C = 6.627 \cdot 10^6$ Nm/rad, $t_0 = 10$ m, $t_1 = 5.0$ s.

For these data, we find the solutions to the minimum values of the denominators of the criterion components (4). As a result of the calculations, we obtain:

$$\min\left(\sqrt{\frac{1}{t_1}\int_0^{t_1} M_{dr}^2\, dt}\right) = 128487 \text{ Nm, } \min\left(\sqrt{\frac{1}{t_1}\int_0^{t_1} \dot{M}_{dr}^2\, dt}\right) = 301029 \text{ Nm/s. The}$$

obtained values are used to normalize the dimensionless components of criterion (4) with weight coefficients δ_1 and δ_2.

4. Results and Discussion

From the obtained solutions, we built graphical dependences of the power (Figs. 2 and 3), energy (Fig. 4), and kinematic (Figs. 5 and 6) features. In addition, estimated values of the slewing mechanism during the startup process at a steady-state trolley movement at different values of the weight coefficients of criterion (4) are calculated (Table 1).
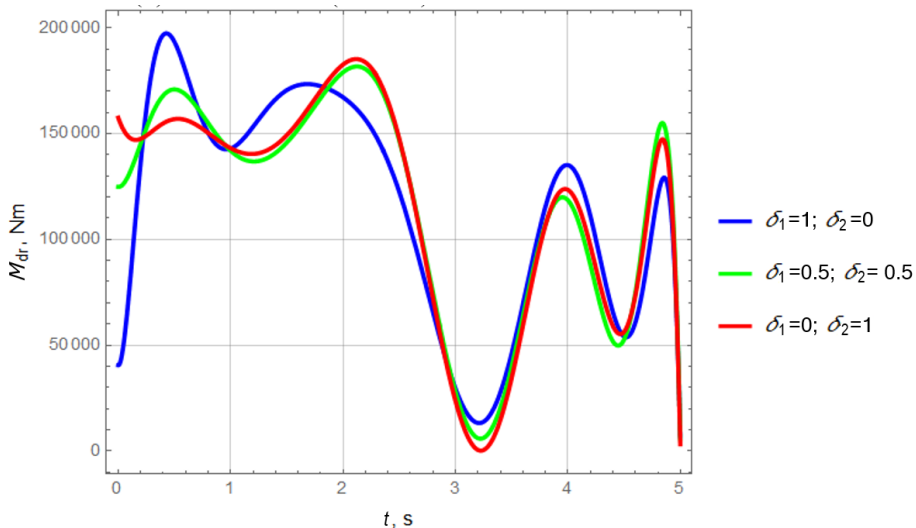

Fig. 2. Plots of the drive torque

The plots in Fig. 2 show that in the first half of the startup the drive torque at different values of the weight coefficients has a different pattern of change, and in
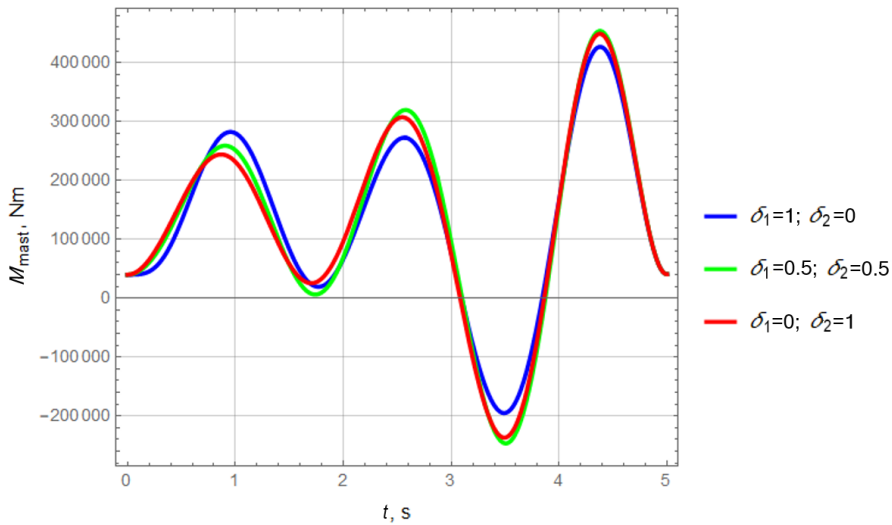
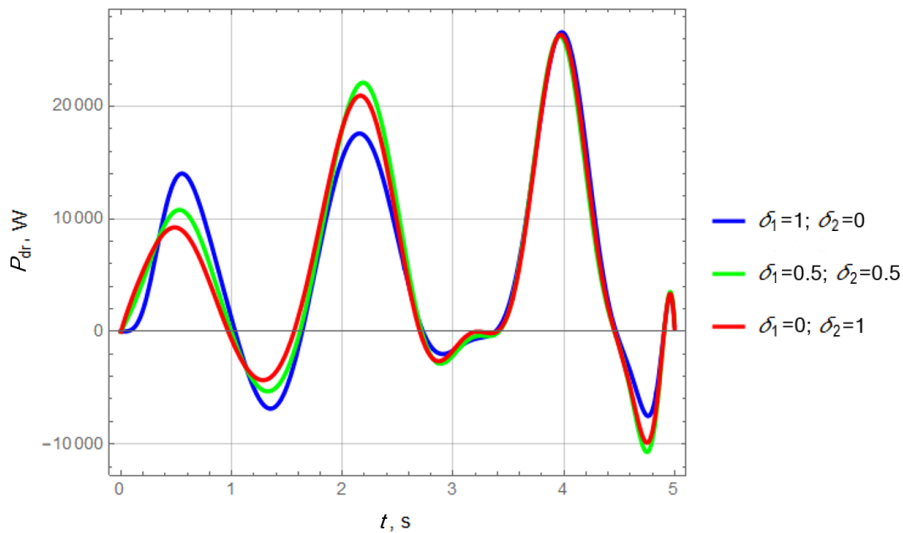Fig. 3. Plots of elastic torque in the crane tower

Fig. 4. Plots of the dynamic power component of the drive

the second half of the startup it changes almost identically. The highest maximum value of the drive torque is observed at the weight coefficients $\delta_1 = 1$, $\delta_2 = 0$ and is about 197.4 kNm. At the other two startup modes, the maximum values are almost the same and reach 181.7 and 185.2 kNm. The RMS values of the drive torque in all three startup modes are almost the same and reach the values close to 57 kNm. The lowest initial starting torque occurs in the mode of motion with weight coefficients $\delta_1 = 1$, $\delta_2 = 0$ and equals 40 kNm, and the highest – at $\delta_1 = 0$, $\delta_2 = 1$ and equals
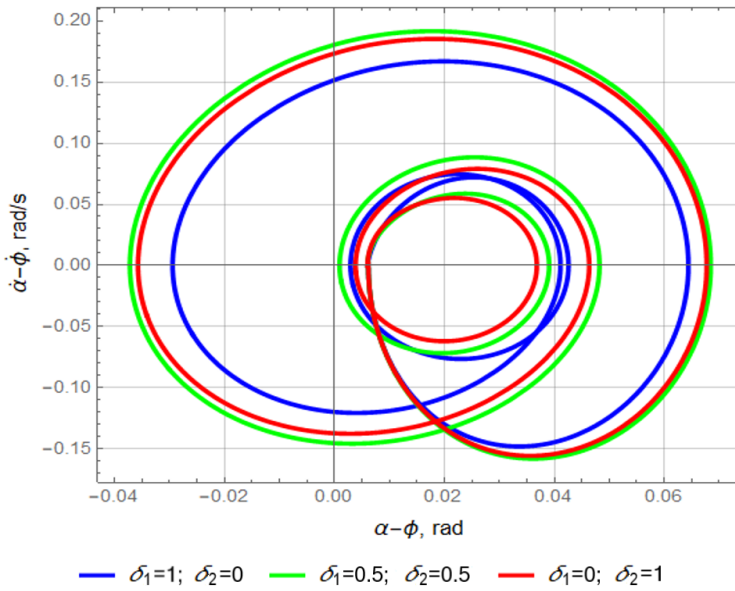
Fig. 5. Phase portrait of the tower elastic oscillations
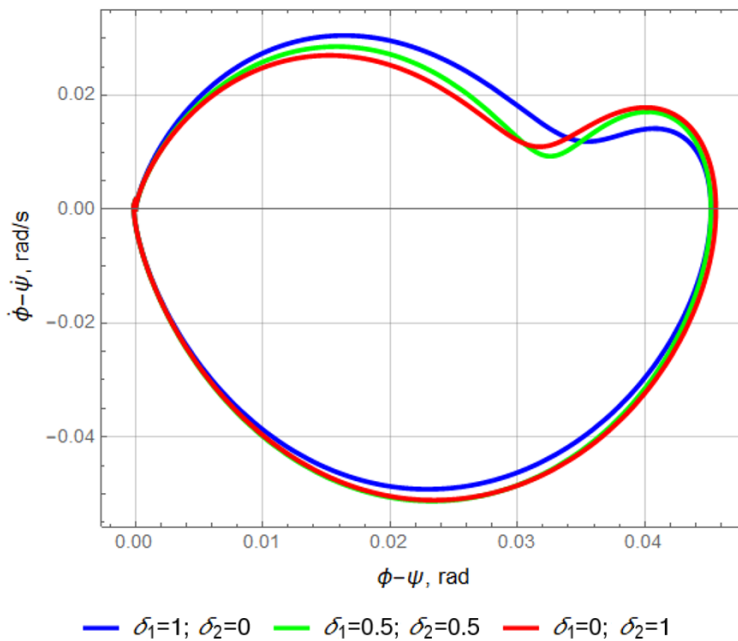

Fig. 6. Phase portrait of the pendulum oscillations of the load

160 kNm. Under the startup mode with weight coefficients $\delta_1 = 0.5$, $\delta_2 = 0.5$ the initial start torque takes an intermediate value of 125 kNm.

Table 1. Estimated indicators of the optimal mode of the tower crane slewing mechanism at different values of weight coefficients

Item No.	Description	Unit of measure	Estimated indicators for the values of weight coefficients		
			$\delta_1 = 1$; $\delta_1 = 0$	$\delta_1 = 0.5$; $\delta_1 = 0.5$	$\delta_1 = 0$; $\delta_1 = 1$
Class of extreme indicators					
1	Maximum value of the drive torque	Nm	197359	181708	185192
2	Minimum value of the drive torque	Nm	7043	5831	193
3	Maximum value of the elastic torque in the tower	Nm	426756	453643	448796
4	Minimum value of the elastic torque in the tower	Nm	−195085	−246537	−236812
5	Maximum value of drive power	W	26561	26234	26347
6	Minimum value of drive power	W	−7499	−10699	−9870
7	Magnitude of the elastic tower deformation	rad	0.0644	0.0684	0.0677
8	Magnitude of load pendulum oscillations	rad	0.0452	0.0452	0.0455
Class of integral indicators					
9	RMS value of the drive torque	Nm	57044	56902	57059
10	RMS value of the torque in the tower	Nm	89916	95983	94188
11	RMS value of drive power	W	4632	4827	4691
12	RMS value of the elastic tower deformation	rad	0.0136	0.0145	0.0142
13	RMS value of the deviation of the rope with a load from the vertical	rad	0.0117	0.0116	0.0116

The pattern of elastic torque in the crane rotary tower changing (Fig. 3) is almost identical at different values of the complex criterion weight coefficients. In this case, the maximum values of the elastic torque in the tower occur at the same time at different values of the weight coefficients. They are almost the same in magnitude. The lowest maximum value corresponds to the startup mode with weight coefficients $\delta_1 = 1$, $\delta_2 = 0$ and equals 426.7 kNm, and the highest – at case $\delta_1 = 0.5$, $\delta_2 = 0.5$ and reaches 453.6 kNm. A similar pattern is observed for the RMS value of the elastic torque in the tower, where the minimum value is in the first mode and the maximum value is in the second mode. They are equal to 89.9 and 96.0 kNm, respectively. In all three startup modes, the elastic torque in the tower has an asymmetric change relative to the time axis.

During the entire startup process, the dynamical component of the drive power (Fig. 4) in different motion modes is described by quite a similar dependencies. However, in the first half of the startup process, there are some deviations in the maximum values of local extremes. Thus, for example, in the first extreme, the biggest maximum power value, is achieved at the weight coefficients $\delta_1 = 1$, $\delta_2 = 0$

in criterion (4) and is 14.5 kW, and the smallest one – at $\delta_1 = 1$, $\delta_2 = 0$ and reaches 9.5 kW. A slightly different picture is observed at the third extreme, where the biggest maximum value is achieved at $\delta_1 = 0.5$, $\delta_2 = 0.5$ and is 22.5 kW, and the smallest one – at $\delta_1 = 1$, $\delta_2 = 0$ and is equal to 17.0 kW. In general, the highest maximum power value occurs at the fifth extreme, which is almost the same for all three startup modes and close to 26.5 kW.

From the phase portrait of the elastic oscillations of the crane tower (Fig. 5), it can be seen that the nature of the oscillations under all three start-up modes is damped and quite similar in waveform. The startup mode at the values of the weight coefficients $\delta_1 = 1$, $\delta_2 = 0$ in criterion (4) provides the lowest maximum values of the deformation (0.0644 rad) and deformation rate (0.165 rad/s) of the tower. The largest deformation (0.0684 rad) and deformation rate (0.190 rad/s) of the tower are achieved in the startup mode with weight coefficients $\delta_1 = 0.5$, $\delta_2 = 0.5$. According to the RMS value of the tower deformation, the mode with $\delta_1 = 1$, $\delta_2 = 0$ (0.0136 rad) is also the best, and the worst one is the mode with $\delta_1 = 0.5$, $\delta_2 = 0.5$ (0.0145 rad).

From the observation of phase portrait of the load pendulum oscillations on a flexible suspension (Fig. 6) it can be concluded that in each of the three considered startup modes, the oscillations are eliminated in one oscillation cycle. This is achieved through the selection of boundary conditions during the startup process. All the three modes of the drive mechanism accelerations provide almost identical phase portraits of load oscillations. The load oscillation magnitude in all three motion modes is almost the same and equals to 0.0452, 0.0452 and 0.0455 rad, respectively. A similar picture is observed in terms of the RMS value of the deviation from the vertical of the load rope with the load. They equal to 0.0117, 0.0116 and 0.0116 rad, respectively.

From the results of the optimization of the slewing mechanism startup mode (Figs. 2–6 and Table 1), it can be concluded that most of the power, energy, and kinematic parameters under different startup modes are quite close to each other. It indicates that, in addition to the criterion, the optimization results are significantly influenced by the boundary conditions of motion and constraints to the power parameters, which are assumed to be the same for the three options of the weight coefficients of the complex criterion.

5. Conclusions

In the article, a dynamical model of the tower crane slewing mechanism under the steady-state mode of trolley movement is developed, on the basis of which the differential equations of motion are derived. On the basis of the obtained equations, an optimization problem is stated and solved according to a complex dimensionless dynamical criterion, which includes the components of the RMS values of the drive torque and the rate of its change over time. The impact of each component of the complex criterion is assessed by weight coefficients that

are varied from 0 to 1. Optimization problems with different values of the weight coefficients are solved with the same constraints $0 \leqslant M_{dr} \leqslant M_{\max.dr}$. The same type of kinematic characteristics of the crane's slewing mechanism are chosen as the boundary conditions of motion, to which additional conditions are added as optimization parameters to find.

Since the optimization problem is nonlinear, a modification of the metaheuristic method VCT-PSO of optimization algorithm is applied to solve it. The obtained optimal start-up modes of the crane slewing mechanism at different values of the weight coefficients ensure minimization of the complex integral dynamical criterion and eliminate low-frequency oscillations of the load on a flexible suspension and high-frequency elastic oscillations of the slewing tower.

The optimization of the crane slewing mechanism startup mode is carried out according to a complex criterion at different values of the weight coefficients under the same constraints imposed on the drive torque and boundary conditions of motion. Based on the results of optimization of the slewing mechanism startup modes, it is found that most of the kinematic, dynamical, and power parameters at different values of the weight coefficients are almost identical or quite close to each other. It indicates that, in addition to the criterion, the results of the optimization are significantly influenced by the boundary conditions of motion and constraints to the power characteristics.

The relevance of the obtained results for a real-world application is in the implementation of the optimal modes of motion via variable frequency drive. Since a great variety of control laws may be implemented with variable frequency drives, the results obtained in the current study aren't exceptional. The drive torque law may be coded in a proper software and written to an on-board microcontroller, which forms commands and sends them to the frequency inverter. It, in turn, changes the frequency and voltage of the drive and the desired (optimal) law $M_{dr}(t)$ is applied to the system.

References

[1] E.M. Abdel-Rahman, A.H. Nayfeh, and Z.N. Masoud. Dynamics and control of cranes: A review. *Journal of Vibration and Control*, 9(7):863–908, 2003. doi: 10.1177/1077546303009007007.

[2] S.C. Kang and E. Miranda. Physics based model for simulating the dynamics of tower cranes. In *2004 Proceeding of Xth International Conference on Computing in Civil and Building Engineering (ICCCBE)*, Weimar, Germany, June 2004. doi: 10.25643/bauhaus-universitaet.240.

[3] T. Kuo, Y-C. Chiang, S-Y. Cheng, and S.-C.J. Kang. Oscillation reduction method for fast crane operation. *Modular and Offsite Construction (MOC) Summit Proceedings*, pages 388–395, 2015. doi: 10.29173/mocs159.

[4] G. Sun and M. Kleeberger. Dynamic responses of hydraulic mobile crane with consideration of the drive system. *Mechanism and Machine Theory*. 38(12):1489–1508, 2003. doi: 10.1016/S0094-114X(03)00099-5.

[5] T. Čampara, H. Bukvić, D. Sprečić. Ability to control swinging of payload during the movement of the rotary cranes mechanism. In *4th International Conference on Intelligent Technologies*

in Logistics and Mechatronics Systems. Kaunas University of Technology Panevezys Institute, pages 52–55, Kaunas. Lithuania, 2009.

[6] V. Loveikin, Yu. Romasevych, A. Loveikin, and M. Korobko. Optimization of the trolley mechanism acceleration during tower crane steady slewing. *Archive of Mechanical Engineering*, 69(3):411–429, 2022. doi: 10.24425/ame.2022.140424.

[7] I. Gutierrez-Carmona and J. Colado. Control of a two wired hammerhead tower crane. *Nonlinear Dynamics*, 84(4):2137–2148, 2016. doi: 10.1007/s11071-016-2634-3.

[8] P. Schlott, F. Rausher, and O. Sawodny. Modelling the structured dynamics of a tower crane. In *2016 IEEE International Conference on Advanced Intelligent Mechatronics (AIM)*, pages 763–768, Banff, Canada, 2016. doi: 10.1109/AIM.2016.7576860.

[9] R.P. Gerasymyak and V.A. Leshchev. *Analysis and Synthesis of Crane Electromechanical Systems*. 2008. (in Russian).

[10] R.P. Gerasymyak and O.V. Naidenko. Features of the control of the electric drive of the boom departure mechanism during the rotation of the crane with a suspended load. *Electrical Engineering and Electrical Equipment*, 68:11–15, 2007. (in Ukrainian).

[11] Naidenko E.V. Electric drive control of horizontal movement mechanisms with a suspended load. *Electric Machine Building and Electric Control*, 69:17–22, 2007.

[12] M. Čolić, N. Pervan, M. Delić, A.J. Muminović, S. Odžak, and V. Hadžiabdić. Mathematical modelling of bridge crane dynamics for the time of non-stationary regimes of working hoist mechanism. *Archive of Mechanical Engineering*, 69(2):189–202, 2022. doi: 10.24425/ame.2022.140415.

[13] S. Chwastek. Optimization of crane mechanism to reduce vibration. *Automation in Construction*, 119:103335, 2020. doi: 10.1016/j.autcon.2020.103335.

[14] V. Loveikin, Yu. Romasevych, A. Loveikin, A. Lyashko,and M. Korobko. Minimization of high frequency oscillations of trolley movement mechanism during steady tower crane slewing. *UPB Scientific Bulletin, Series D: Mechanical Engineering*, 84(1):31-44, 2022.

[15] Z. Liu, T. Yang, N. Sun, and Y. Fang. An antiswing trajectory planning method with state constraints for 4-DOF tower cranes: Design and experiments. *IEEE Access*, 7: 62142–62151, 2019. doi: 10.1109/ACCESS.2019.2915999.

[16] T.K. Nguyen. Combination of feedback control and spring-damper to reduce the vibration of crane payload. *Archive of Mechanical Engineering*, 68(2):165–181, 2021. doi: 10.24425/ame.2021.137046.

[17] G. Rigatos, M. Abbaszadeh, and J. Pomares. Nonlinear optimal control for the 4-DOF underactuated robotic tower crane. *Autonomous Intelligent Systems*, 2:21, 2022. doi: 10.1007/s43684-022-00040-4.

[18] A. Al-Fadhli and E. Khorshid. Payload oscillation control of tower crane using smooth command input. *Journal of Vibration and Control*, 29(3-4):902–915. 2023. doi: 10.1177/10775463211054640.

[19] S.-J. Kimmerle, M. Gerdts, and R. Herzog. An optimal control problem for a rotating elastic crane-trolley-load system. *IFAC-PapersOnLine*, 51(2):272-277, 2018, doi: 10.1016/j.ifacol.2018.03.047.

[20] Y. Romasevych, V. Loveikin, and Y. Loveikin. Development of a PSO modification with varying cognitive term. *2022 IEEE 3rd KhPI Week on Advanced Technology, KhPI Week 2022 – Conference Proceedings*, Kharkiv, Ukraine, 2022. doi: 10.1109/KhPIWeek57572.2022.9916413.